Fuel 289 (2021) 119939

Contents lists available at ScienceDirect

Fuel

journal homepage: www.elsevier.com/locate/fuel

Full Length Article

# Effect of additives on the oxidative stability and corrosivity of biodiesel samples derived from babassu oil and residual frying oil: An experimental and theoretical assessment

Nelly V.P. Rangel [a], Leonardo P. da Silva [b], Vinícius S. Pinheiro [a], Igor M. Figueredo [a,e], Othon S. Campos [c], Stefane N. Costa [d], Francisco Murilo T. Luna [e], Célio L. Cavalcante Jr. [e], Emmanuel S. Marinho [f], Pedro de Lima-Neto [b], Maria A.S. Rios [a,*]

[a] Grupo de Inovações Tecnológicas e Especialidades Químicas, Centro de Tecnologia, Universidade Federal do Ceará, Campus do Pici, Bloco 714, CEP 60440-554 Fortaleza, CE, Brazil
[b] Departamento de Química Analítica e Físico-Química, Centro de Ciências, Universidade Federal do Ceará, Campus do Pici, Bloco 940, CEP 60440-900 Fortaleza, CE, Brazil
[c] Departamento de Química e Física, Universidade Federal do Espírito Santo, Campus Guararema, CEP 29500-000 Alegre, ES, Brazil
[d] Programa de Pós-Graduação em Engenharia Metalúrgica e de Materiais, Universidade Federal do Ceará, Fortaleza, CE, Brazil
[e] Grupo de Pesquisa em Separações por Adsorção, Núcleo de Pesquisas em Lubrificantes, Departamento de Engenharia Química, Universidade Federal do Ceará, Fortaleza, CE CEP 60455-900, Brazil
[f] Faculdade de Filosofia Dom Aureliano Matos, Universidade Estadual do Ceará, CEP 62930-000 Limoeiro do Norte, Ceará, Brazil

ARTICLE INFO

*Keywords:*
FUKUI index
DFT
PDA
IONOL
Hydrogenated cardanol

ABSTRACT

The objective of this work is to evaluate the effect of the addition of N,N′-di-*sec*-butyl-p-phenylenediamine (PDA), IONOL, and hydrogenated cardanol (HC) (500 mg/kg, each) on the oxidative stability and corrosivity of biodiesel obtained from babassu oil (BB) and from residual frying oil (BRFO). Oxidative stability was assessed by induction period (IP) using the Rancimat method (EN 14112), while the corrosivity was assessed by the mass losses of copper coupons immersed in the biodiesel samples (ASTM TM0169/G31-12a (2010)). The most severe corrosion was observed for the fresh biodiesel samples without any additives (4.85 mpy for BB, and 5.00 mpy for BRFO). Using PDA, IONOL, and HC as additives inhibited the copper corrosion in both biodiesel samples (between 0.61 and 3.09 mpy for BB, and between 2.19 and 4.69 mpy for BRFO). The use of IONOL and PDA as additives, besides showing a decrease in corrosion rates, also improved the oxidative stability (IP values) for both biodiesel samples (by 66 and >100 h, for BB; and by 3.31 and 7.23 h, for BRFO, respectively), demonstrating that these additives have bi-functionality in these biodiesel samples. Conversely, the use of HC increased the oxidative stability for BB (by 10.82 h) but also presented a pro-oxidant effect on biodiesel obtained from residual frying oil, decreasing its IP value by *ca.* 18%. Finally, theoretical studies were carried out based on the formalism of the functional density theory, which confirmed that PDA has indeed the highest anti-corrosion potential among the studied additives.

## 1. Introduction

The gradual depletion of fossil fuel reserves, the increase of oil prices, and environmental concerns have accelerated the need to find fuels that meet technical and sustainable requirements given the consequences of the greenhouse effect on human health. In this perspective, based on the principles of green chemistry for the use of renewable energies, biodiesel has stood out as an alternative to petrodiesel. This fuel is biodegradable and may be produced from different fatty raw materials [1,2].

Considered environmentally friendly because it is sulfur-free, non-toxic, and derived from renewable sources, biodiesel is however susceptible to oxidation, and this represents one of the biggest challenges in its production and commercialization [3]. In the production of biodiesel, triacylglycerols are converted into esters by transesterification to obtain a fuel that has properties similar to petrodiesel [4]. Among the main advantages, it possesses higher flash point than petrodiesel, which facilitates its transport [5], is biodegradable, and generates fewer emissions [6].

However, due to its chemical structure and the presence of double

* Corresponding author.
*E-mail address:* alexsandrarios@ufc.br (M.A.S. Rios).

https://doi.org/10.1016/j.fuel.2020.119939
Received 20 August 2020; Received in revised form 28 November 2020; Accepted 1 December 2020
Available online 16 December 2020

**Nomenclature**

| | |
|---|---|
| A | Electron affinity |
| ABNT NBR | Brazilian Association of Standard Techniques (Portuguese acronym) |
| ASTM | American Society for Testing and Materials |
| BB | Babassu Biodiesel |
| BRFO | Biodiesel produced from Residual Frying Oil |
| CNSL | Cashew Nut Shell Liquid |
| CR | Corrosion Rate (mpy) |
| D | Density (kg/m$^3$) |
| DFT | Functional Density Theory |
| EN | European Standards |
| FAME | Fatty acid methyl esters |
| $f_k$ | Condensed Fukui Functions |
| HC | hydrogenated cardanol |
| HOMO | Highest Occupied Molecular Orbital |
| I | Ionization potential |
| IP | Induction Period (h) |
| $IP_{Ad}$ | Induction Period of the doped samples with antioxidants (h) |
| $IP_{orig}$ | Induction Period of samples without antioxidants (h) |
| LUMO | Lowest Occupied Molecular Orbital |
| PDA | N,N′-di-*sec*-butyl-p-phenylenediamine |
| $q_k$ | Atomic Hirshfeld charge |
| RANP | Resolution of the National Agency of Petroleum, Natural Gas and Biofuels |
| S | exposed area (m$^2$) |
| SF | Stabilization Factor |
| t | immersion time (h) |
| TAN | Total Acid Number |
| w | weight loss (kg) |
| ΔE | Energy gap (eV) |
| $\Delta f$ | dual descriptor |
| ΔN | transferred electron fraction |
| Δω | net electrophilicity (eV) |
| μ | electronical chemical potential |
| η | global hardness (eV/mol) |
| ω | global electrophilicity index (eV) |
| $\omega^-$ | electrodonating (eV) |
| $\omega^+$ | electroaccepting (eV) |
| χ | electronegativity (eV) |

bonds in the carbon chains, biodiesel is susceptible to oxidation that happens without the need of external factors [2]. Its degree of degradation and corrosivity depends on a set of variables that include the fatty acids composition, storage conditions, and external factors such as light, heat, oxygen, humidity, and contact with metals [7].

In addition, the presence of unsaturated compounds, water, and free fatty acids may impact the oxidative stability of biodiesel. Unsaturated esters with bis-allylic methylene groups adjacent to the double bond are very unstable under elevated temperature and/or pressure conditions in the presence of oxygen [8]. Consequently, the original fatty acids content in the feedstock shall impact the stability of the obtained biodiesel, i.e., more saturated feedstocks will yield more stable biodiesel products, as observed in several previous reports [1,3,7,8]. High water content in biodiesel may also intensify the oxidation rate and microbial growth in storage tanks, which could lead to the corrosion of metals [9]. As biodiesel oxidation propagates, there is an increase in properties like acidity index, peroxide value and viscosity, while iodine value and content of methyl esters decrease thus affecting the quality of the final biodiesel product [10].

The initial stage of the oxidation process promotes the formation of primary products, and in sequence, by the reaction of hydroperoxides, the secondary products such as ketones, acids, polymers, volatile products, and species of high molecular weight are formed [11]. These acid compounds accelerate the oxidative degradation of biodiesel, and consequently, the corrosion of metal surfaces [12].

Several studies indicate that the corrosivity of biodiesel can be reduced by using antioxidants [13,14]. These additives act inhibiting the oxidative degradation of biodiesel samples, and consequently, the formation of acid compounds. In addition, these compounds have other applications such as support for fluidity, reduction of NOx emissions, and increasing of lubricity [15–17].

Antioxidants may be classified in natural and synthetic groups. In substitution or associated with synthetic antioxidants, the natural additives may be a sustainable and affordable alternative to increase the oxidative stability of biodiesel [17–26]. Rodrigues et al. (2020) [27] reported that the natural ethanolic extract of turmeric (*Curcuma longa* Linn) showed the best response in the control of the oxidative process of biodiesel of Tilapia oil compared to three synthetic antioxidants that were studied (butylated hydroxyl anisole, butylated hydroxyl toluene, and propyl gallate). Rial et al. (2020) [28] also reported the effect of the addition of an ethanolic extract of cagaita leaf on soybean biodiesel and confirmed its antioxidant potential.

Besides the experimental procedures, theoretical studies were carried out based on the formalism of the functional density theory to simulate the anti-corrosion effects of the investigated antioxidant molecules. These computational tools have gained reliability and applicability with the use of more comprehensive and robust mathematical models [29–31] and were used in this study to correlate the calculated molecular properties of the antioxidants with the experimental results obtained for oxidative stability and corrosion. The use of simulation models would allow reduction in production costs and support the development of strategic scenarios for optimal addition of antioxidants in the biodiesel industry.

In this study, the oxidative stability and corrosivity of biodiesel samples obtained from babassu oil and from residual frying oil were evaluated by the Rancimat method (EN 14112) and by the ASTM TM0169/G31-12a (2010) method, respectively. The effects of the addition of three antioxidants in both samples were also evaluated by the same techniques, aiming to observe the bi-functionality of these additives. Furthermore, the reactivity of those additives was assessed through molecular modeling using functional density theory (DFT).

## 2. Experimental section

### 2.1. Pre-treatment and characterization of raw materials

The residual frying oil was collected in a polyethylene container from a local market in Fortaleza, Brazil. The pre-treatment of the raw material was carried out in four steps: first, the oil was filtered to remove solid particles; second, the liquid phase was heated to 65 °C and washed with 5% g/g of distilled water under continuous stirring; third, the sample was dried under vacuum at 100 °C, for 30 min, using a rotatory evaporator (Buchi, Switzerland); finally, the oil phase was filtered using $Na_2SO_4$ to remove any residual water.

The babassu coconut oil was acquired in the central market in Teresina, Brazil. The acidity indexes of both oil samples were determined following the titration method EN 14104:2003.

### 2.2. Biodiesel production

Both biodiesel samples were obtained through the transesterification reaction of the original oils with analytical grade methanol (99.8%) at

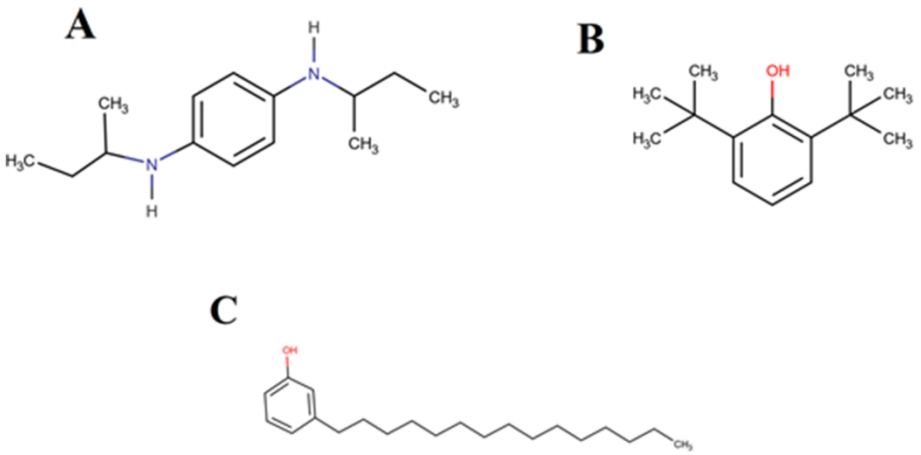


**Fig. 1.** Molecular structures of PDA (A), IONOL (B), and hydrogenated cardanol (C).

1:6 (oil/alcohol) molar ratio, using potassium hydroxide (KOH, 85%) as a catalyst. The experimental apparatus consisted of a three-neck round-bottom flask connected to a reflux condenser. The temperature of the reaction systems was kept at 60 ± 5 °C, under continuous stirring, following a procedure reported by Serrano et al. (2014) [32].

The biodiesel from the residual frying oil (BRFO) was obtained by transesterification of the pre-treated sample for 60 min using 1.73 wt% of KOH. After the reaction, the ester phase and glycerol were separated in a funnel at room temperature. The ester phase was washed three times with 10% vol. of distilled water, at 60 °C. Additional washing steps were carried out with distilled water at room temperature until the washing water reached neutral pH. Finally, the ester phase was dried by heating to 90 ± 5 °C for 20 min, under continuous stirring, and filtered with sodium sulfate anhydrous to remove any water residue.

For the synthesis of babassu biodiesel (BB), a two-step transesterification was applied following a previously reported methodology [33]. At the first step, the babassu oil was reacted with methanol, using 0.5 wt% of KOH, for 60 min. Then, the fatty acid methyl esters (FAME) and glycerol were separated in a funnel at room temperature. At the second step, the ester phase reacted with methanol, using 0.26 wt% of KOH, for 30 min, totalizing 0.76 wt% of catalyst. After that, the products were transferred to a funnel, separating the glycerol from the ester phase, also at room temperature. The washing and filtering processes were carried out exactly as for the synthesis of BRFO.

### 2.3. Physicochemical characterization of the obtained biodiesel samples

Density at 20 °C was determined using a digital densimeter (Anton Paar DMA 4500, USA) with an accuracy of 1 x$10^{-5}$ g/$cm^3$ following Brazilian method NBR14065:2013. The kinematic viscosity was measured using a glass capillary kinematic viscometer according to Brazilian method ABNT NBR 10441:2014. The moisture content was performed using a Karl-Fischer coulometric equipment following ASTM D6304:2007 (831 KF Coulometer, Metrohm, Switzerland). The Total Acid Number (TAN) was measured according to EN 14104:2003.

### 2.4. Additives

The additives used in this study were hydrogenated cardanol (HC), IONOL and N,N′-di-*sec*-butyl-p-phenylenediamine (PDA). HC (3-pentadecylphenol), a natural phenolic antioxidant derived from the processing of Cashew Nut Shell Liquid (CNSL), was supplied by Sigma-Aldrich (technical grade, 90% wt.). A further purification, using a chromatographic column with silica gel (average pore size 60 Å (52–73 Å), 70–230 mesh) and hexane (99% wt.) as eluent, was carried on to obtain a powder with purity ≥99% wt. IONOL is a mixture of phenolic compounds, mainly 2,6-ditert-butylphenol (57.5% wt.), 2,4,6-tris-tertbutylphenol (18.7% wt.) and other phenolic molecules, supplied by Sigma-Aldrich (>99% wt.). PDA (98% wt.) was kindly provided by Chemtura (USA).

### 2.5. Oxidative stability measurements

The oxidative stability was evaluated using a Rancimat apparatus (Metrohm, model 873, Switzerland) according to EN 14112. The effluent air from the sample was bubbled through a vessel containing deionized water, where the absorption of oxidation volatile products causes an increase in conductivity. The change in conductivity values are used to estimate the induction period (IP), which is determined by the maximum of the second derivative of the curve of conductivity *versus* time. The stabilizing factor (SF) is used to report the effectiveness of an antioxidant in retarding the oxidation of biodiesel and is calculated using Equation (1) [7,34].

$$SF = IP_{Ad}/IP_{orig} \quad (1)$$

where $IP_{Ad}$ is the IP of the biodiesel sample doped with antioxidant, and $IP_{orig}$ is the IP of the fresh biodiesel sample (without antioxidant).

### 2.6. Corrosion tests

The corrosion immersion tests were performed following ASTM TM0169/G31-12a, at room temperature (≅ 30 °C) for 720 h, by immersion of copper coupons (rectangular cubic shape (1.97; 0.91; 0.47 cm)) in both biodiesel samples, with and without additives. The samples of babassu oil biodiesel (BB) and biodiesel of residual frying oil (BRFO) were doped with HC, IONOL, and PDA (500 mg/kg, each).

Before use, each copper coupon was polished using silicon carbide papers, then rinsed in distilled water and degreased with acetone. For the tests, the coupons were immersed in beakers containing 210 mL of biodiesel samples. The weight loss of the coupons after the immersion for 720 h was used to calculate the corrosion rate with Equation (2), according to Fazal et al. (2018) [2]:

$$CR = 8.76x10^9 w/DtA \quad (2)$$

In this equation, *CR* is the corrosion rate in mils-per-year (mpy); w is the weight loss of the Cu coupon in kg; D is the density of the copper in kg/$m^3$; A is the exposed area of the coupon, in $m^2$ and t is the immersion time in h.

### 2.7. Gas chromatography

The ester content was measured using gas chromatography (Varian, GC 450 model, Palo Alto, CA), according to Brazilian method ABNT

15764. Summary of Test Method: capillary column CP-Wax 52 CB (30 m, 0.25 μm film thickness, 0.32 mm i.d.); injection volumes of 0.5 μL and 1.0 μL; temperatures (injector, oven, and detector) of 250, 170, and 390 °C, respectively; nitrogen flow rate of 28 mL/min and methyl nonadecanoate (C19:0) as an internal standard.

### 2.8. Molecular modeling

The structures of the molecules (PDA, IONOL and HC, see Fig. 1) were optimized at the DFT level, with the functional and basic set M06-2X / 6–311 + G (d, p), respectively [35]. All quantum calculations were performed in the Gaussian 09 program package in vacuum at 298.15 K [36]. All frequencies were checked for the absence of negative vibrational frequencies. The chemical reactivity of the PDA, IONOL and HC molecules were predicted by the following parameters: HOMO energy, LUMO energy, energy gap (ΔE), ionization potential (I), electron affinity (A), electronical chemical potential (μ), electronegativity (χ), global hardness (η), global electrophilicity index (ω), electroaccepting ($\omega^+$), electrodonating ($\omega^-$), Net electrophilicity (Δω) (Eqs. (3)–(12)) [37–39].

The transferred electron fraction (ΔN) between the copper and the antioxidants molecules were calculated according to Equation (13), where $\chi_{Cu}$ and $\eta_{Cu}$ are electronegativity and hardness of copper, respectively, while $\chi_{inh}$ and $\eta_{inh}$ are the corresponding molecular properties for the antioxidant molecules.

$$\Delta E_{gap} = E_{LUMO} - E_{HOMO} \tag{3}$$

$$I = -E_{HOMO} \tag{4}$$

$$A = -E_{LUMO} \tag{5}$$

$$\mu = \frac{I + A}{2} \tag{6}$$

$$\chi = -\mu = \frac{I + A}{2} \tag{7}$$

$$\eta = \frac{I - A}{2} \tag{8}$$

$$\omega = \frac{\mu^2}{4\eta} = \frac{\chi^2}{4\eta} \tag{9}$$

$$\omega^- = \frac{(3I + A)^2}{16(I - A)} \tag{10}$$

$$\omega^+ = \frac{(I + 3A)^2}{16(I - A)} \tag{11}$$

$$\Delta\omega = \omega^+ - \omega^- \tag{12}$$

$$\Delta N = \frac{\chi_{Cu} - \chi_{inh}}{2(\eta_{Cu} + \eta_{inh})} \tag{13}$$

To complete the local reactive characterization, the dual descriptor (Δ*f*), (Eqs. (14)–(17)) were computed at the same level of theory [40]. The isosurface of the Electronic Fukui functions was computed in the Multiwfn software and visualized using the VESTA program [41,42].

$$f_k^+ = q_k(N+1) - q_k(N) \tag{14}$$

$$f_k^- = q_k(N) - q_k(N-1) \tag{15}$$

$$f_k^o = \frac{q_k(N+1) - q_k(N-1)}{2} \tag{16}$$

$$\Delta f = f_k^+ - f_k^- \tag{17}$$

**Table 1**
Physicochemical properties of BB and BRFO.

| Property | BB* | BRFO** | Limits*** | Method |
|---|---|---|---|---|
| Acidity index (mg KOH/g), max | 0.20 | 0.28 | 0.50 | EN 14104 |
| Density, 20 °C (kg/m$^3$) | 871 | 885 | 850–900 | ASTM 4052 |
| Kinematic viscosity, 40 °C (mm$^2$/s) | 2.8 | 4.8 | 3.0–6.0 | EN 3104 |
| Moisture content (mg/kg), max | 0.3 | 0.2 | 200 | EN 12937 |
| Ester content (%), min | 98.0 | 96.6 | 96.5 | EN 14103 |
| Induction period (h), min | 4.4 | 4.1 | 12 | EN 14112 |

* Babassu biodiesel, ** Biodiesel of Residual Frying Oil, *** RANP 45/2014 [43].

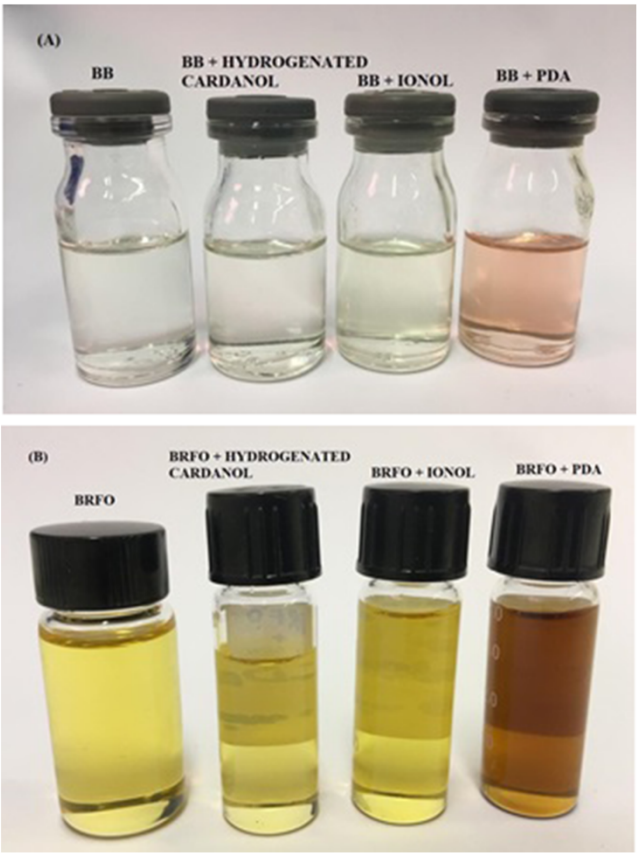


**Fig. 2.** Photographic images of (A) BB without antioxidants, BB + hydrogenated cardanol, BB + IONOL, and BB + PDA; and (B) BRFO without antioxidants, BRFO + hydrogenated cardanol, BRFO + IONOL, and BB + PDA. All doped samples have the same concentration of antioxidant (500 mg/kg, each).

## 3. Results and discussion

### 3.1. Physicochemical properties

The acidity indexes of the oil samples were 0.68 mg KOH/g for babassu oil and 1.1 mg KOH/g for residual frying oil. The main physicochemical properties of the obtained biodiesel samples (BB and BRFO) are shown in Table 1, along with the Brazilian specifications [43]. Most properties met the regulatory limits, except for the kinematic viscosity at 40 °C of BB and the induction period (IP) for both BB and BRFO. It is also possible to highlight that BB presented a higher ester content, lower acidity index, and lower kinematic viscosity when compared to BRFO.

### 3.2. Effect of the additives on oxidative stability of BB and BRFO

The photographic images of fuel samples, including all doped samples, at 500 mg/kg, are presented in Fig. 2. The effect of the addition of

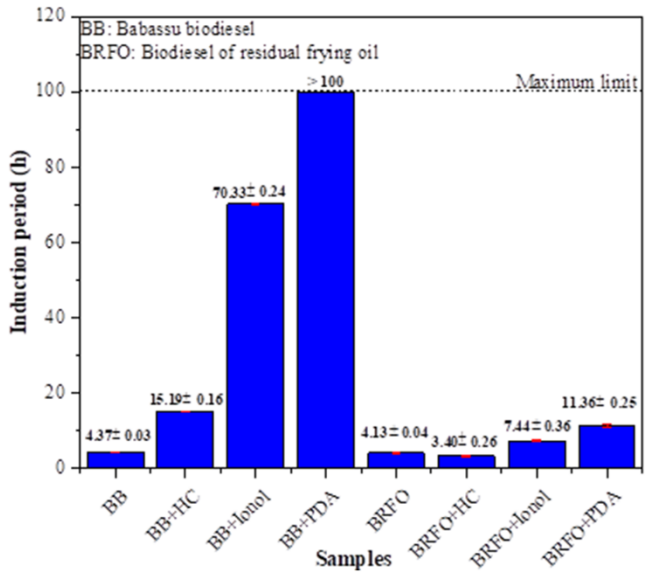


**Fig. 3.** Effect of hydrogenated cardanol (HC), IONOL, and PDA (500 mg/kg, each) on the oxidative stability of BB and BRFO.

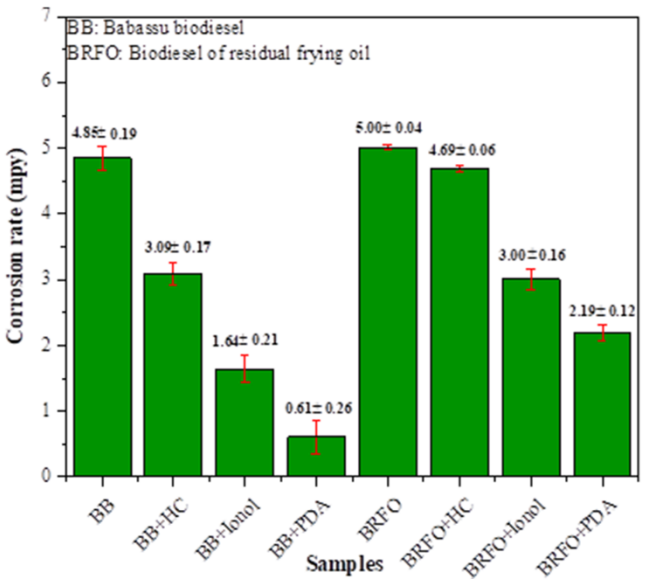


**Fig. 4.** Corrosion rate of copper coupons immersed in BB and BRFO with and without hydrogenated cardanol, IONOL, and PDA (500 mg/kg, each). All test samples were maintained at room temperature (≅30 °C) for 30 days.

HC, IONOL, and PDA (500 mg/kg, each) on the oxidative stability of babassu biodiesel (BB) and biodiesel of residual frying oil (BRFO) is shown in Fig. 3. It was observed that, for the babassu biodiesel, all additives promoted increments in the induction period (IP), with PDA showing the best antioxidant performance. For the biodiesel produced from residual frying oil, HC acted as a pro-oxidant, its addition reduced the induction period of BRFO by 17.7% (0.73 h), whereas IONOL and PDA increased the IP by 80.1% and 175.1%, respectively. In general, it may seen in Fig. 3 that all additives had better performance when added to the BB sample than when added to the BRFO sample.

The higher oxidative stability of the BB and the effectiveness of the additives in this biodiesel might be attributed to the high content of saturated fatty acids (>85%), especially lauric acid (C12:0), associated to the presence of α-tocopherol, the predominant natural antioxidant in the babassu oil [17,44–48]. Since the chemistry of biodiesel depends on the fatty oil from which it is derived, its stability increases with increasing content of saturated fatty acid of the feedstock [17]. HC, IONOL, and PDA increased the induction period of BB by 250% (10.82 h), 1500% (66 h), and >2200% (>100 h), respectively. These results proved the remarkable potential of PDA, an antioxidant of the class of secondary amines [43], to improve the oxidative stability of babassu biodiesel.

The stages involved in an oxidation process are initiation, propagation, and termination. According to the oxidation stage in which antioxidants act, they might be classified as primary or secondary antioxidants. Primary antioxidants act as chain breaking, interrupting the propagation stage of the oxidation through hydrogen atom donation (O–**H** or N–**H**) to free radicals. This group includes HC, IONOL, and PDA. Secondary antioxidants act on the elimination of free radicals and decomposition of hydroperoxides, transforming them into stable products [17,49].

The PDA molecule contains two NH groups (see Fig. 1) that may react with peroxy radicals, while both IONOL and HC have only one OH group. The number of donating groups influences the antioxidant activity. Compounds with two donating groups shall be more effective than a compound with only one. This characteristic might explain the better performance of PDA [33].

In contrast, the BRFO sample and its formulations (BRFO + additive) showed much lower induction periods (none of them reaching the Brazilian regulatory limit of 12 h), which might be attributed to the significant presence of free fatty acids. The frying process in cooking oil takes place at high temperatures (~160–220 °C), in which natural or synthetic antioxidants might be degraded. Besides, the factors oxygen, temperature, and humidity favour the oxidation of the oil contributing to the break of carbon chains, and increased viscosity, acidity index, and peroxide value. Also, its direct interaction with food and metals might further increase the degradation process of the oil that is submitted to frying [50–52].

The high acidity index of the residual frying oil (1.1 mg KOH/g) might also have contributed to the low efficiency of the additives with the BRFO sample, because this index may interfere on the result of Rancimat, since this method monitors the increase in conductivity of the deionized water, which absorbs acid compounds [7,46,50–52].

### 3.3. Corrosion tests

The corrosion rates obtained calculated from the copper coupons immersed in the babassu biodiesel (BB) and in the biodiesel of residual frying oil (BRFO), with and without additives (HC, IONOL, and PDA, 500 mg/kg each), are shown in Fig. 4.

It may be seen that the copper coupons immersed in BRFO showed a higher corrosion rate than those immersed in BB (5.00 and 4.85 mpy, respectively). It was also observed that all additives reduced the corrosion rates of the coupons. In the BB sample, HC, IONOL, and PDA reduced the corrosion rate by 36% (1.8 mpy), 66% (3.2 mpy), and 87% (4.2 mpy), respectively. On the other hand, for the BRFO samples, the addition of HC, IONOL, and PDA reduced the corrosion rate by 6% (0.3 mpy), 40% (2.0 mpy), and 56% (2.8 mpy), respectively. Thus, the effectiveness of the additives in both biodiesel samples followed the order: PDA > IONOL > HC.

Amine inhibitors protect against corrosion mainly through adsorption on the metal surface and nitrogen bonding via pi electrons [53]. The antioxidant effect of phenolic compounds is related to the electron donating nature and the steric effect of the substituent, in which the steric effect prevents the coupling of the phenoxy radicals and increases the number of peroxyl radicals retained. The electron donor effect may increase the electron density in the phenol oxygen, resulting in a high rate of radical retention [54].

According to some authors [2,11], copper acts as a catalyst in reducing monounsaturated esters when it interacts with biodiesel forming different acid compounds and short chain molecules. This is due

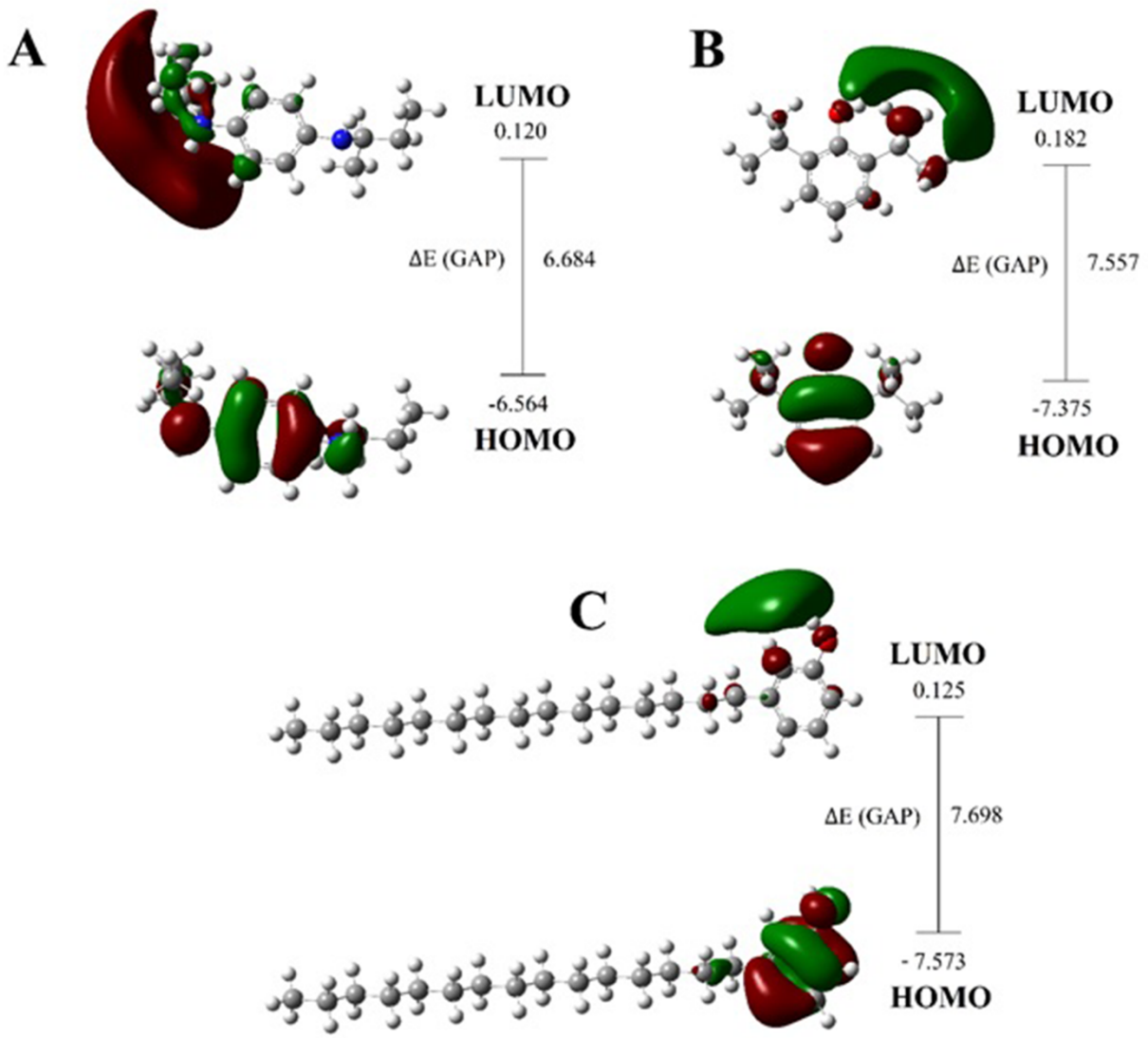


**Fig. 5.** HOMO and LUMO images, and E (gap) of the neutral structures of PDA (A), IONOL (B), and hydrogenated cardanol (C), calculated at the M06-2X/6–311 + G (d, p) level of theory.

to double bonds of the original fatty acid, which provide reaction sites for the metal ions. Thus, since BRFO is composed mainly of short and monounsaturated chains [46,50,55], higher degradation, and consequent corrosivity to copper, can be expected, which is clearly evident from the higher corrosion rates observed for the samples evaluated using this biodiesel.

### 3.4. Modeling results

#### 3.4.1. Global reactivity

The concepts of Koopman's Theorem are associated with the energy of the boundary orbitals to describe the chemical reactivity of the molecule, and it is observed that this is related to the adsorption experiment of molecules on metallic surface [56,57]. In global chemical reactivity, electronic affinity is addressed with the LUMO orbital (empty orbital with less energy). In the ionic potential, it is described as the energy to remove the electron, in which it can be seen the relationship with the HOMO orbital, which is the occupied orbital with the highest energy [37].

The energy needed to excite the electron from the HOMO orbital to the LUMO orbital is namely, gap energy. Fig. 5 shows the HOMO, LUMO, and E (gap) of the neutral structures of PDA (A), IONOL (B), and HC (C) in mediums at M06-2X/6–311 + G (d, p). The PDA obtained the lowest index of $\Delta E = 6.684$ eV, which indicates a great advantage in terms of global reactivity. The IONOL and HC obtained $\Delta E = 7.556$ eV and $\Delta E = 7.698$ eV, respectively. The higher electronegativity of HC ($\chi = 3.724$ eV) indicates the greatest tendency to attract electrons [39]. In the electrophilicity, indicates the tendency of molecular stabilization when

**Table 2**
Quantum reactivity chemical parameters for PDA, IONOL, and HC using the DFT methods M06-2X/6–311 + G (d, p).

| Molecule | I | A | η | ΔE | χ | ω | ω+ | ω- | Δω | ΔN |
|---|---|---|---|---|---|---|---|---|---|---|
| PDA | 6.564 | −0.120 | 3.342 | 6.684 | 3.222 | 1.553 | 0.360 | 3.582 | 3.942 | 0.188 |
| IONOL | 7.375 | −0.182 | 3.779 | 7.557 | 3.597 | 1.712 | 0.386 | 3.982 | 4.368 | 0.117 |
| HC | 7.573 | −0.125 | 3.849 | 7.698 | 3.724 | 1.802 | 0.421 | 4.145 | 4.565 | 0.098 |

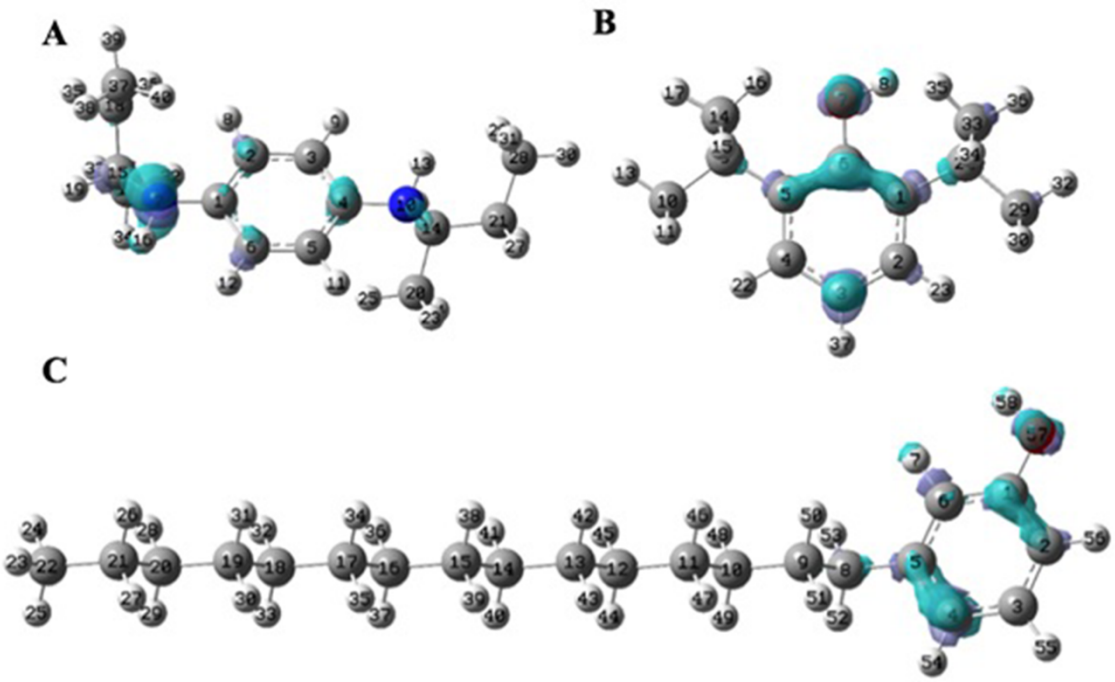


**Fig. 6.** The isosurface density of the Fukui function from Δf for PDA (A), IONOL (B), and hydrogenated cardanol (C).

receiving external electrons [58], with HC showing a higher value of ω = 1.802 eV.

The quantum reactivity chemical parameters for PDA, IONOL, and HC using the DFT methods M06-2X/6–311 + G (d, p) are shown in In Table 2. HC obtained the highest ω (1.802 eV), which represents its susceptibility to accept electrons, and thus, is the best electrophile in comparison to PDA and IONOL. In contrast, PDA showed the lowest ω (1.553 eV) being the best nucleophile.

In the ΔN index, the fraction of electrons transferred to the surface (Equation (13)) [59], the copper electronegativity can be defined as $\chi_{Cu}$ = 4.48 eV and the copper hardness as $\eta_{Cu}$ = 0 eV/mol. According to results, PDA presented the higher ΔN (0.188) being the best electron donor for the surface compared to the other additives. The data indicate that due to the global reactivity, the PDA presents the greatest reactivity in comparison to HC and IONOL.

The molecules were also compared through of the electroaccepting and electrodonating powers described by the indices $\omega^+$ and $\omega^-$, respectively. A high value of $\omega^+$ indicates a greater tendency for the molecule to accept charge, while a lower value of w- indicates a greater tendency to donate charge [60]. Therefore, HC with a value of 0.421 eV, showed a better tendency to receive charge, while with a value of 3.582 eV in $\omega^-$, PDA showed to have the best tendency in charge donation. And to ascertain the liquid electrophilicity, the descriptor $\Delta\omega$ was used, which indicates the general trend between donation and reception of charge, following Eq. (12), thus indicating that HC has greater liquid electrophilicity.

### 3.4.2. *Mathematical correlations between quantum descriptors and experimental data*

After obtaining the experimental results (Fig. 4), and data from the molecular descriptors in Table 2, mathematical correlations between calculated and experimental data were performed on linear, exponential, and logarithmic scales, to ascertain what molecular properties of the additives are related with the corrosion inhibition of the copper. The $R^2$ is the parameter used to ascertain the effectiveness of each correlation.

For BB, the best correlations were obtained in Net electrophilicity $\Delta\omega$ ($R^2 = 0.9932$), Electrophilicity $\omega$ ($R^2 = 0.999$), and Electroaccepting $\omega^+$ ($R^2 = 0.9999$). On the other hand, electrophicility descriptor displayed the best in linear scale, while the others two best descriptors obtained a better trend in exponential scale. For (BRFO), the best descriptors were Net electrophilicity $\Delta\omega$($R^2 = 0.9078$), Electrophicility $\omega$($R^2 = 0.9349$), and Electroaccepting $\omega^+$ ($R^2 = 0.9998$), where all descriptors obtained the best trends described in exponential scale (see Supplementary material: Fig. S1 and Table S1).

The BB molecules showed the best mathematical correlations between the quantum descriptors and the corrosion rate when compared to the trends in BRFO. The data show that corrosion rate has in its nature a connection with the descriptor $\omega^+$, following an directly proportional trend, with a linear scale, in which, the lower the molecule's characteristic in receiving the charge, the greater its characteristic tendency to be a good anticorrosive.

For correlations with the induction period, the best trends in BB were Net Electrophilicity $\Delta\omega$ ($R^2 = 0.8622$), Electrophilicity $\omega$($R^2 = 0.8951$), Electroaccepting $\omega^+$ ($R^2 = 0.9928$). In BRFO, the descriptor Net electrophilicity $\Delta\omega$ ($R^2 = 0.9535$), Electrophilicity ($\omega$, $R^2 = 0.9724$) and the best index, Electroaccepting $\omega^+$ ($R^2 = 0.9968$), were obtained (Supplementary material Fig. S2, Table S2, and Table S3). The correlations of the quantum descriptors in correlation with the induction period obtained a better trend ($R^2$) on a linear scale except for the descriptor $\omega^+$ which obtained the best mathematical correlation on the logarithmic scale. As well as the correlations of the corrosion rate, the data show that $\omega^+$ follows as the best quantum descriptor, in which there is an inversely proportional logic, wherein this case on the logarithmic scale. Showing that the lower your tendency to receive electrons, the better your characteristic tendency to be a good antioxidant.

### 3.4.3. *Local reactivity*

Based on the local Fukui functions, it possible to obtain the nucleophilic ($f^-$) and electrophilic ($f^+$) sites indicated in Equations (14) and (15), respectively (see Supplementary Material: Tables S4, S5, and S6,) [61]. In the study of the anticorrosive properties of the additives, it was observed a tendency more nucleophilic, which favors adsorption in the metal surface due to the donation of electrons to the surface [62].

Using the electronic density difference, based on the ratio of the variation of the electronic density by the variation of electrons, it can be

calculated the condensed Fukui function of each molecule, obtaining the densities Δf (Fig. 6). Hirshfeld charges were used for the Fukui index.

Therefore, the Δf index was used, which indicates the general trend between donation ($\Delta f < 0$) and electron reception ($\Delta f > 0$) of the atoms. According to the index Δf (see Tables S4, S5, and S6), the atoms 2C, 4C, and N7 for PDA; 3C, 6C, and O7 for IONOL, and 2C, 4C, and O57 for HC contribute significantly to the nucleophilic character of these additives (Fig. 6).

## 4. Conclusions

Babassu oil and residual frying oil may be used as feasible feed stocks to produce biodiesel, since most of their physicochemical properties have complied with the requirements of the Brazilian standard (RANP 45/2014). Additives, initially evaluated as antioxidants, may also be used to reduce the corrosion rate on copper coupons exposed to babassu biodiesel and to biodiesel of residual frying oil. All copper coupons exhibited a high corrosion rate in the absence of the additives. PDA was the most effective additive, increasing the oxidative stability and mitigating the corrosion rate of the coupons for both biodiesel samples.

The presence of IONOL also showed a positive effect in reducing the corrosion rate and increasing the oxidative stability of the biodiesel samples. However, HC presented an anti-corrosive effect on the copper coupons immersed in the BRFO but a pro-oxidant effect reducing the oxidative stability of this biodiesel. Along with the experimental results, theoretical data were obtained by DFT. Based on reactivity parameters, PDA showed the best performance as antioxidant and anti-corrosive, followed by IONOL and HC. This same trend had been observed in the experimental studies. These results confirm the bi-functionality of PDA and IONOL as antioxidants and anticorrosive agents in biodiesel.

## Declaration of Competing Interest

The authors declare that they have no known competing financial interests or personal relationships that could have appeared to influence the work reported in this paper.

## Acknowledgments

This work was supported by CNPq (459355/2014-7, 406697/2013-2, 308280/2017-2); FUNCAP (AEP-00128-00220.01.00/17, DEP-0164-00195.01.00/19), and CAPES (Finance Code 001). Stefane N. Costa and Leonardo P. da Silva thank CAPES for their scholarships. Pedro de Lima-Neto thanks the financial support received from CNPq (304152/2018-8). The authors also thanks Centro Nacional de Processamento de Alto Desempenho (CENAPAD) of the Federal University of Ceará (UFC) for providing computational resources.

## Appendix A. Supplementary data

Supplementary data to this article can be found online at https://doi.org/10.1016/j.fuel.2020.119939.

## References

[1] Altun S. Effect of the degree of unsaturation of biodiesel fuels on the exhaust emissions of a diesel power generator. Fuel 2014;117:450–7. https://doi.org/10.1016/j.fuel.2013.09.028.
[2] Fazal MA, Suhaila NR, Haseeb ASMA, Rubaiee S, Al-Zahrani A. Influence of copper on the instability and corrosiveness of palm biodiesel and its blends: An assessment on biodiesel sustainability. J Clean Prod 2018;171:1407–14. https://doi.org/10.1016/j.jclepro.2017.10.144.
[3] Knothe G, Van Gerpen J, Krahl J, editors. The Biodiesel Handbook. 2nd ed. Urbana (IL): Academic Press and AOCS Press; 2010.
[4] Kaul S, Saxena RC, Kumar A, Negi MS, Bhatnagar AK, Goyal HB, et al. Corrosion behavior of biodiesel from seed oils of Indian origin on diesel engine parts. Fuel Process Technol 2007;88:303–7. https://doi.org/10.1016/j.fuproc.2006.10.011.
[5] Agarwal AK, Gautam A, Sharma N, Singh AP. Introduction of methanol and alternate fuel economy. In: Agarwal AK, Gautam A, Sharma N, Singh AP, editors. Methanol and the alternate fuel economy. Singapore: Springer; 2019. p. 3–6.
[6] Ramalingam S, Rajendran S, Ganesan P, Govindasamy M. Effect of operating parameters and antioxidant additives with biodiesels to improve the performance and reducing the emissions in a compression ignition engine – A review. Renew Sustain Energy Rev 2018;81(Pt 1):775–88. https://doi.org/10.1016/j.rser.2017.08.026.
[7] Sousa LS, Moura CVR, Moura EM. Influence of binary, ternary and quaternary mixtures on oxidative stability and study of kinetics and thermodynamic parameters of the degradation process of soybean biodiesel. Fuel 2020;259:116235. https://doi.org/10.1016/j.fuel.2019.116235.
[8] Fu J, Hue BTB, Turn SQ. Oxidation stability of biodiesel derived from waste catfish oil. Fuel 2017;15:455–63. https://doi.org/10.1016/j.fuel.2017.04.067.
[9] Fregolente PBL, Fregolente LV, Maciel MRW. Water Content in Biodiesel, Diesel, and Biodiesel-Diesel Blends. J Chem Eng Data 2012;57(6):1817–21. https://doi.org/10.1021/je300279c.
[10] Zuleta EC, Baena L, Rios LA, Calderon JA. The oxidative stability of biodiesel and its impact on the deterioration of metallic and polymeric materials: a review. J Braz Chem Soc 2012;23(12):2159–75. https://doi.org/10.1590/S0103-50532012001200004.
[11] Fazal MA, Jakeria MR, Haseeb ASMA. Effect of copper and mild steel on the stability of palm biodiesel properties: A comparative study. Ind Crops Prod 2014;58:8–14. https://doi.org/10.1016/j.indcrop.2014.03.019.
[12] Thangavelu SK, Piraiarasi C, Ahmed AS, Ani FN. Corrosion Behavior of Copper in Biodiesel-Diesel-Bioethanol (BDE). Adv Mater Res 2015;1098:44–50. https://doi.org/10.4028/www.scientific.net/AMR.1098.44.
[13] Almeida ES, Portela FM, Sousa RMF, Daniel D, Terrones MGH, Richter EM, et al. Behaviour of the antioxidant tert-butylhydroquinone on the storage stability and corrosive character of biodiesel. Fuel 2011;90(11):3480–4. https://doi.org/10.1016/j.fuel.2011.06.056.
[14] Deyab MA. Corrosion inhibition of aluminum in biodiesel by ethanol extracts of Rosemary leaves. J Taiwan Inst Chem Eng 2016;58:536–41. https://doi.org/10.1016/j.jtice.2015.06.021.
[15] Kumar N. Oxidative stability of biodiesel: Causes, effects and prevention. Fuel 2017;190:328–50. https://doi.org/10.1016/j.fuel.2016.11.001.
[16] Rashed MM, Masjuki HH, Kalam MA, Alabdulkarem A, Imdadul HK, Rashedul HK, et al. A comprehensive study on the improvement of oxidation stability and $NO_x$ emission levels by antioxidant addition to biodiesel blends in a lightduty diesel engine. RSC Adv 2016;6:22436–46. https://doi.org/10.1039/C5RA26271B.
[17] Varatharajan K, Pushparani DS. Screening of antioxidant additives for biodiesel fuels. Renew Sustain Energy Rev 2018;82(Pt 3):2017–28. https://doi.org/10.1016/j.rser.2017.07.020.
[18] Alberici RM, Simas RC, Abdelnur PV, Eberlin MN, Souza V, Sá GF, et al. A Highly Effective Antioxidant and Artificial Marker for Biodiesel. Energy Fuels 2010;24:6522–6. https://doi.org/10.1021/ef100968b.
[19] Almeida L, Hidalgo A, Vega M, Rios M. Utilização de compostos derivados da biomassa para solução de problemas industriais no setor de biocombustíveis. Estud Tecnol Eng 2012;7(2):163–76. Portuguese.
[20] Chen YH, Chen JH, Luo YM. Complementary biodiesel combination from tung and medium-chain fatty acid oils. Renew Energy 2012;44:305–10. https://doi.org/10.1016/j.renene.2012.01.098.
[21] Kleinberg MN, Rios MAS, Buarque HLB, Parente MMV, Cavalcante Jr CL, Luna FMT. Influence of Synthetic and Natural Antioxidants on the Oxidation Stability of Beef Tallow Before Biodiesel Production. Waste Biomass Valor 2019;10:797–803. https://doi.org/10.1007/s12649-017-0120-x.
[22] Maia FJN, Ribeiro FWP, Rangel JHG, Lomonaco D, Luna FMT, Lima-Neto P, et al. Evaluation of antioxidant action by electrochemical and accelerated oxidation experiments of phenolic compounds derived from cashew nut shell liquid. Ind Crops Prod 2015;67:281–6. https://doi.org/10.1016/j.indcrop.2015.01.034.
[23] Paiva GMS, Freitas AR, Nobre FX, Leite CMS, Matos JME, Rios MAS. Kinetic and thermal stability study of hydrogenated cardanol and alkylated hydrogenated cardanol. J Therm Anal Calorim 2015;120:1617–25. https://doi.org/10.1007/s10973-015-4528-x.
[24] Rios MAS, Santiago SN, Lopes AAS, Mazzetto SE. Antioxidative activity of 5-n-pentadecyl-2-tert-butylphenol stabilizers in mineral lubricant oil. Energy Fuels 2010;24:3285–91.
[25] Rios MAS, Santos FFP, Maia FJN, Mazzeto SE. Evaluation of antioxidants on the thermo-oxidative stability of soybean biodiesel. J Therm Anal Calorim 2013;112:921–7. https://doi.org/10.1007/s10973-012-2650-6.
[26] Rodrigues MG, Souza AG, Santos IMG, Bicudo TC, Silva MCD, Sinfrônio FSN, et al. Antioxidative Properties of Hydrogenated Cardanol for Cotton Biodiesel by PDSC and UV/VIS. J Therm Anal Calorim 2009;97(2):605–9.
[27] Rodrigues JS, Valle CP, Uchoa AFJ, Ramos DM, Ponte FAF, Rios MAS, et al. Comparative study of synthetic and natural antioxidants on the oxidative stability of biodiesel from Tilapia oil. Renew Energy 2020;156:1100–6. https://doi.org/10.1016/j.renene.2020.04.153.
[28] Rial RC, Merlo TC, Santos PHM, Melo LFD, Barbosa RA, Freitas ON, et al. Evaluation of oxidative stability of soybean methyl biodiesel using extract of cagaite leaves (Eugenia dysenterica DC.) as additive. Renew. Energy 2020;152:1079–85.. https://doi.org/10.1016/j.renene.2020.01.121.
[29] Davis SC, Anderson-Teixeira KJ, DeLucia EH. Life-cycle analysis and the ecology of biofuels. Trends Plant Sci 2009;14(3):140–6. https://doi.org/10.1016/j.tplants.2008.12.006.

[30] Perimenis A, Walimwipi H, Zinoviev S, Müller-Langer F, Miertus S. Development of a decision support tool for the assessment of biofuels. Energy Policy 2011;39(3):1782–93. https://doi.org/10.1016/j.enpol.2011.01.011.
[31] Kikolski M. Study of production scenarios with the use of Simulation Models. Procedia Eng 2017;182:321–8. https://doi.org/10.1016/j.proeng.2017.03.102.
[32] Serrano M, Oliveros R, Sanchez M, Moraschini A, Martinez M, Aracil J. Influence of blending vegetable oil methyl esters on biodiesel fuel properties: Oxidative stability and cold flow properties. Energy 2014;65:109–15. https://doi.org/10.1016/j.energy.2013.11.072.
[33] Figueredo IM, Rios MAS, Cavalcante Jr CL, Luna FMT. Effects of amine and phenolic based antioxidants on the stability of Babassu Biodiesel using Rancimat and Differential Scanning Calorimetry Techniques. Ind Eng Chem Res 2019;59(1):18–24. https://doi.org/10.1021/acs.iecr.9b05209.
[34] Chen YH, Luo YM. Oxidation stability of biodiesel derived from free fatty acids associated with kinetics of antioxidants. Fuel Process Technol 2011;92(7):1387–93. https://doi.org/10.1016/j.fuproc.2011.03.003.
[35] Zhao Y, Truhlar DG. The M06 suite of density functionals for main group thermochemistry, thermochemical kinetics, noncovalent interactions, excited states, and transition elements: Two new functionals and systematic testing of four M06-class functionals and 12 other function. Theor Chem Acc 2008;120:215–41. https://doi.org/10.1007/s00214-007-0310-x.
[36] Frisch MJ, Trucks GW, Schlegel HB, Scuseria GE, Robb MA, Cheeseman JR, et al. Gaussian 09, Revision B.01. Gaussian 09, Revis. B.01, Gaussian, Inc., Wallingford CT; 2009.
[37] Koopmans T. Uber die Zuordnung von Wellenfunktionen und Eigenwerten zu den Einzelnen Elektronen Eines Atoms. Physica 1934;1(1–6):104–13. German.
[38] Parr RG, Pearson RG. Absolute hardness: companion parameter to absolute electronegativity. J Am Chem Soc 1983;105(26):7512–6. https://doi.org/10.1021/ja00364a005.
[39] Chermette H. Chemical reactivity indexes in density functional theory. J Comput Chem 1999;20(1):129–54. https://doi.org/10.1002/(SICI)1096-987X(19990115)20:1<129::AID-JCC13>3.0.CO;2-A.
[40] Fukui K. Role of frontier orbitals in chemical reactions. Science 1982;218(4574):747–54. https://doi.org/10.1126/science.218.4574.747.
[41] Lu T, Chen F. Multiwfn: A multifunctional wavefunction analyzer. J Comput Chem 2012;33(5):580–92. https://doi.org/10.1002/jcc.22885.
[42] Momma K, Izumi F. VESTA 3 for three-dimensional visualization of crystal, volumetric and morphology data. J Appl Crystallogr 2011;44(Pt 6):1272–6. https://doi.org/10.1107/S0021889811038970.
[43] ANP. National Agency of Petroleum, Natural Gas and Biofuels. Resolution 45/2014, [acessed 18 August 2020].
[44] Paula RSF, Figueredo IM, Vieira RS, Nascimento TL, Cavalcante CL, Machado YL, et al. Castor–babassu biodiesel blends: estimating kinetic parameters by Differential Scanning Calorimetry using the Borchardt and Daniels method. SN Appl Sci 2019;1:884. https://doi.org/10.1007/s42452-019-0917-2.
[45] Barthi R, Singh B. Green tea (Camellia assamica) extract as an antioxidant additive to enhance the oxidation stability of biodiesel synthesized from waste cooking oil. Fuel 2020;262:116658. https://doi.org/10.1016/j.fuel.2019.116658.
[46] Camargo RPL, Carrim AJI, Franco PIBM, Antoniosi Filho NR. Assessment of the physicochemical suitability of oils and frying fats residuals for biodiesel production. Waste Tech 2016;4(2):1–8. https://doi.org/10.12777/wastech.4.2.1-8.
[47] Santos DS, Silva IG, Araujo BQ, Lopes Jr CA, Monçao NBN, Cito AMGL, et al. Extraction and evaluation of Fatty Acid compositon of Orbignya phalerata Martius Oils (Arecaceae) from Maranhão State. Brazil. J Braz Chem Soc 2013;24(2):355–62. https://doi.org/10.5935/0103-5053.20130045.
[48] Serra JL, Rodrigues AMC, Freitas RA, Meirelles AJA, Darnet SH, Silva LHM. Alternative sources of oils and fats from Amazonian plants: Fatty acids, methyl tocols, total carotenoids and chemical composition. Food Res Int 2019;116:12–9. https://doi.org/10.1016/j.foodres.2018.12.028.
[49] Dunn RO. Antioxidants for improving storage stability of biodiesel. Biofuels Bioprod Bioref 2008;2(4):304–18. https://doi.org/10.1002/bbb.83.
[50] Shaban SA. Biodiesel production from waste cooking oil. Egypt J Chem 2012;55(5):437–52. https://doi.org/10.21608/ejchem.2012.1167.
[51] Sanibal EAA, Mancini Filho J. Perfil de Ácidos Graxos Trans de Óleo e Gordura Hidrogenada de Soja no Processo de Fritura. Cienc Tecnol Aliment 2004;24(1):27–31., Campinas, 24(1):27-31. Portuguese.
[52] Freire PCM, Mancini Filho J, Ferreira TAPC. Principais alterações físico-químicas em óleos e gorduras submetidos ao processo de fritura por imersão: regulamentação e efeitos na saúde. Rev Nutr 2013;26(3):353–68. Portuguese.
[53] Rihan R, Shawabkeh R, Al-Bakr N. The Effect of Two Amine-Based Corrosion Inhibitors in Improving the Corrosion Resistance of Carbon Steel in Sea Water. J Materi Eng Perform 2014;23:693–9. https://doi.org/10.1007/s11665-013-0790-x.
[54] Al-Sehemi AG, Irfan A. Effect of donor and acceptor groups on radical scavenging activity of phenol by density functional theory. Arab J Chem 2017;10(Suppl 2):S1703–10. https://doi.org/10.1016/j.arabjc.2013.06.019.
[55] Predojević ZJ, Škrbić BD. Alkali-catalyzed production of biodiesel from waste frying oils. J Serbian Chem Soc 2009;74(8–9):993–1007. https://doi.org/10.2298/JSC0909993P.
[56] Wazzan NA. DFT calculations of thiosemicarbazide, arylisothiocynates, and 1-aryl-2,5-dithiohydrazodicarbonamides as corrosion inhibitors of copper in an aqueous chloride solution. J Ind Eng Chem 2015;26:291–308. https://doi.org/10.1016/j.jiec.2014.11.043.
[57] Verma C, Olasunkanmi LO, Bahadur I, Lgaz H, Haque QMA, J,, et al. Experimental, density functional theory and molecular dynamics supported adsorption behavior of environmental benign imidazolium based ionic liquids on mild steel surface in acidic medium. J Mol Liq 2019;273:1–15. https://doi.org/10.1016/j.molliq.2018.09.139.
[58] Parr RG, Szentpály LV, Liu S. Electrophilicity index. J Am Chem Soc 1999;121(9):1922–4. https://doi.org/10.1021/ja983494x.
[59] Pearson RG. Absolute Electronegativity and Hardness: Application to Inorganic Chemistry. Inorg Chem 1988;27(4):734–40. https://doi.org/10.1021/ic00277a030.
[60] Gázquez JL, Cedillo A, Vela A. Electrodonating and Electroaccepting Powers. J Phys Chem A 2007;111(10):1966–70. https://doi.org/10.1021/jp065459f.
[61] Singh P, Ebenso EE, Olasunkanmi LO, Obot IB, Quraishi MA. Electrochemical, Theoretical, and Surface Morphological Studies of Corrosion Inhibition Effect of Green Naphthyridine Derivatives on Mild Steel in Hydrochloric Acid. J Phys Chem C 2016;120(6):3408–19. https://doi.org/10.1021/acs.jpcc.5b11901.
[62] Nwankwo HU, Olasunkanmi LO, Ebenso EE. Experimental, quantum chemical and molecular dynamic simulations studies on the corrosion inhibition of mild steel by some carbazole derivatives. Sci Rep 2017;7:2436. https://doi.org/10.1038/s41598-017-02446-0.